Journal of Thrombosis and Haemostasis, **12**: 1–10 DOI: 10.1111/jth.12705

ORIGINAL ARTICLE

Factor XIII stiffens fibrin clots by causing fiber compaction

N. A. KURNIAWAN,* J. GRIMBERGEN,† J. KOOPMAN† and G. H. KOENDERINK*
**FOM Institute AMOLF, Amsterdam; and †ProFibrix BV, Leiden, the Netherlands*

To cite this article: Kurniawan NA, Grimbergen J, Koopman J, Koenderink GH. Factor XIII stiffens fibrin clots by causing fiber compaction. *J Thromb Haemost* 2014; DOI: 10.1111/jth.12705.

Summary. *Background:* Factor XIII-induced cross-linking has long been associated with the ability of fibrin blood clots to resist mechanical deformation, but how FXIII can directly modulate clot stiffness is unknown. *Objectives and Methods:* We hypothesized that FXIII affects the self-assembly of fibrin fibers by altering the lateral association between protofibrils. To test this hypothesis, we studied the cross-linking kinetics and the structural evolution of the fibers and clots during the formation of plasma-derived and recombinant fibrins by using light scattering, and the response of the clots to mechanical stresses by using rheology. *Results:* We show that the lateral aggregation of fibrin protofibrils initially results in the formation of floppy fibril bundles, which then compact to form tight and more rigid fibers. The first stage is reflected in a fast (10 min) increase in clot stiffness, whereas the compaction phase is characterized by a slow (hours) development of clot stiffness. Inhibition of FXIII completely abrogates the slow compaction. FXIII strongly increases the linear elastic modulus of the clots, but does not affect the non-linear response at large deformations. *Conclusions:* We propose a multiscale structural model whereby FXIII-mediated cross-linking tightens the coupling between the protofibrils within a fibrin fiber, thus making the fiber stiffer and less porous. At small strains, fiber stiffening enhances clot stiffness, because the clot response is governed by the entropic elasticity of the fibers, but once the clot is sufficiently stressed, the modulus is independent of protofibril coupling, because clot stiffness is governed by individual protofibril stretching.

Keywords: blood coagulation; elasticity; factor XIII; fibrin; turbidimetry.

Correspondence: Gijsje H. Koenderink, FOM Institute AMOLF, Science Park 104, 1098XG Amsterdam, the Netherlands.
Tel.: +31 20 7547100; fax: +31 20 7547290.
E-mail: gkoenderink@amolf.nl

Received 13 May 2014
Manuscript handled by: T. Lisman
Final decision: P. H. Reitsma, 13 August 2014

Introduction

Fibrin is a fibrous biopolymer that serves as the structural scaffold in blood clots. Clots form when fibrinogen, a 340-kDa glycoprotein consisting of three pairs of polypeptide chains $(A\alpha B\beta\gamma)_2$, is enzymatically converted to fibrin monomers that self-assemble into branched fibrous networks [1]. Factor XIII is a pro-transglutaminase that, when activated, is responsible for introducing covalent bonds between the α-chains and γ-chains of fibrin monomers, thereby stabilizing fibrin clots against degradation [2]. The cross-linking introduced by FXIII has a pronounced effect on the mechanical properties of the clot, increasing the clot stiffness two-fold to five-fold [3,4]. Patients with a deficiency in FXIII generally suffer from severe hemorrhagic diathesis, whereas more common mutations or polymorphisms have been associated with either an increased or a decreased risk of thrombosis [2,5], as fibrin networks have a crucial mechanical role in preventing clots from being dislodged or damaged by the dynamic shear of blood flow [6]. How exactly FXIII can directly affect fibrin clot stiffness, however, is currently unclear.

FXIII can, in principle, alter the structure of the fibrin network, by modulating the density of cross-linking between fibers, and/or affect the fibrin fibers themselves. Previous studies have shown that the clot architecture in terms of fiber branching and mesh size is minimally affected by FXIII [4,7]. Furthermore, manipulation of individual fibrin fibers with atomic force microscopy and of fibers inside a clot with optical tweezers has demonstrated that FXIII-mediated cross-linking enhances both the tensile and flexural stiffness of individual fibers [4,8,9]. From these lines of evidence, we hypothesized that FXIII stiffens clots primarily by causing changes within the fibers themselves, as the fibers are hydrated bundles of protofibrils with variable packing density [10]. To test this hypothesis, we quantitatively analyzed the kinetics of fibrin clotting in terms of molecular cross-linking, fiber assembly, and clot stiffness, with a focus on the role of FXIII in clot maturation and mechanical function.

Materials and methods

Fibrinogen samples and fibrin formation

Human plasma-derived fibrinogen depleted of plasminogen, von Willebrand factor and fibronectin from Enzyme Research Laboratories (Swansea, UK) was dissolved in water and dialyzed against Hepes-buffered saline (HBS) buffer (20 mM Hepes, 150 mM NaCl, pH 7.4). The preparation contained FXIII, as judged by the presence of bands indicating α-cross-linked and γ-cross-linked chains on reducing SDS polyacrylamide gels after thrombin-mediated conversion to fibrin, as described below. Recombinant fibrinogen (rFib610), possessing intact α-chains with a length of 610 amino acids, corresponding to the main constituent of plasma fibrinogen, was expressed in human PER.C6 cells, purified from cell culture supernatant, and dialyzed against HBS buffer [11]. Human FXIII was obtained in zymogen form from Enzyme Research Laboratories. 1,3-Dimethyl-4,5-diphenyl-2-[(2-oxopropyl)thio]imidazolium, trifluorosulfonic acid salt (D004), a specific inhibitor of FXIII [12], was obtained from Zedira (Darmstadt, Germany), and dissolved in dimethylsulfoxide (DMSO) to a concentration of 20 mM.

All fibrin clots were polymerized at a fibrinogen concentration of 2 mg mL^{-1} and at a temperature of 37 °C, in a buffer of pH 7.4 containing 23 mM Hepes, 2 mM $CaCl_2$, and 175 mM NaCl, with 1 NIH U mL^{-1} human α-thrombin (Enzyme Research Laboratories). In experiments involving FXIII inhibition, we added D004 just before adding thrombin. As the D004 compound was dissolved in DMSO, which may affect the structure of the assembled network [13], we used the same final amount of DMSO (1% v/v) in all samples containing D004 and in the control samples. Control turbidimetry experiments on rFib610 clots confirmed that there are no off-target effects of D004 on polymerization kinetics and fibrin structure (Fig. S1). Cross-linked rFib610 clots were obtained by adding purified FXIII in zymogen form to the fibrinogen solutions just before adding thrombin.

Cross-linking analysis by SDS-PAGE

The degree of covalent cross-linking of the fibrin clots was analyzed with reducing SDS-PAGE. Clot formation of samples containing 2 mg mL^{-1} fibrinogen, 1 NIH U mL^{-1} thrombin, 0–20 μg mL^{-1} FXIII and 0–200 μM D004 was initiated by the addition of thrombin and incubation at 37 °C. The reaction was terminated at the indicated time points by the addition of SDS-PAGE sample buffer (Sigma Aldrich, Zwijndrect, the Netherlands) and heating at 95 °C for 10 min. Samples holding the equivalent of 3 μg of fibrinogen per lane were run on 8% polyacrylamide gels. The gels were then stained with InstantBlue (Gentaur, Eersel, The Netherlands) and scanned. Densitometry analysis of the images was performed with a custom-written script in MATLAB (The MathWorks, Natick, MA, USA).

Rheometry

Rheological measurements were performed on a stress-controlled rheometer (MCR 501; Anton Paar, Graz, Austria) equipped with a steel cone-plate geometry (1°, 30 mm). Fibrin samples were assembled *in situ* by transferring the fibrinogen solution immediately upon the addition of thrombin onto the preheated (37 °C) bottom plate. Sample evaporation was prevented by coating the sample edges with mineral oil. Polymerization of the samples was monitored for 4 h by applying an oscillatory shear strain with an amplitude of 0.5% and frequency of 0.5 Hz, and recording the elastic modulus, G', and the viscous modulus, G''. To study the mechanical response of fibrin clots at high shear stress, we employed a differential prestress protocol [14], whereby a constant prestress τ was applied to the sample, and the differential stiffness at this prestress value, $K'(\tau)$, was measured by superimposing a small oscillatory shear stress with an amplitude of 0.1τ and a frequency of 0.5 Hz. All measurements were performed at 37 °C.

Turbidimetry

Turbidimetry analysis provides quantitative information on the diameter and mass/length ratio of individual fibers in the clot by measuring the scattered light intensity as a function of wavelength [10,15]. For a suspension of randomly oriented, long and thin cylindrical fibers with diameter d, the turbidity, t, is: $t\lambda^5 = A\mu(\lambda^2 - Br^2)$, where $t = D\ln(10)$, $A = (88/15)c\pi^3 n_s (dn/dc)^2 (1/N_A)$, and $B = (184/231)\pi^2 n_s^2$. Here, D is the optical density, N_A is Avogadro's number, n_s is the refractive index of the solvent, dn/dc is the specific refractive index increment ($dn/dc = 0.17594$ cm^3 g^{-1} for fibrin [10]), μ is the mass/length ratio of the fibers, and c is the protein concentration expressed in g mL^{-1}. By plotting $t\lambda^5$ against λ^2 and fitting a linear function, the average fiber radius, r, and diameter, $d = 2r$, can therefore be obtained. The number of protofibrils per fiber, N_p, relates to μ through $N_p = \mu/\mu_0$, where $\mu_0 = 1.44 \times 10^{11}$ Da cm^{-1} is the protofibril mass/length ratio [16]. On the assumption that the fibers have a cylindrical shape, fiber density can be calculated as $\mu(\pi r^2)^{-1}$ [17]. Note that here fiber density represents the specific density of the fibers, which reflects the intrafibrillar structure, and is not to be confused with the number density of fibers in the clot.

Immediately after the addition of thrombin, fibrinogen solutions were transferred to quartz cuvettes (1-cm path length; Hellma Analytics, Müllheim, Germany), sealed with air-tight caps to prevent evaporation, and placed in a Lambda 35 spectrophotometer (Perkin Elmer, Groningen, the Netherlands), with the temperature set at 37 °C.

For the time course of polymerization, the absorbance value at 350 nm was continuously monitored. For turbidimetry analysis, wavelength scans were carried out in the range of 500–800 nm every 2.2 min for 4 h of polymerization. Data analysis was performed with a custom-written MATLAB code (Fig. S2).

Confocal imaging

For network visualization with confocal fluorescence microscopy, fibrinogen was labeled with Oregon Green 488 isothiocyanate mixed isomers (Invitrogen, Bleiswijk, the Netherlands), and mixed with unlabeled fibrinogen in a 1 : 10 molar ratio. Samples were prepared in sealed glass chambers and polymerized at 37 °C for 4 h before imaging. Confocal imaging was performed on a Nikon Eclipse Ti inverted microscope equipped with a 100 × oil immersion lens (numerical aperture of 1.49), a 488-nm laser (Coherent, Utrecht, The Netherlands) for illumination, and a photomultiplier tube detector (A1; Nikon, Amsterdam, the Netherlands). The gain and offset were initially adjusted to prevent camera saturation, and were subsequently fixed for all images.

Statistical analysis

All values quoted in this study are means ± standard deviations; *P*-values were determined with Student's *t*-test, and *n*-values are indicated.

Results

Fibrin clotting involves fiber compaction

FXIII is known to cross-link fibrin fibers by forming intermolecular γ-glutamyl–ε-lysyl covalent bonds between the C-terminal portions of the γ-chains, between the α-chains, and between the γ-chains and α-chains [2,18], although the specific longitudinal or transverse arrangements of these cross-links are still debated [19,20]. To reveal the kinetics of cross-linking, we performed reducing SDS-PAGE of plasma-derived fibrin clots terminated at different time points during fibrin formation, up to 4 h (Fig. 1A). Fibrinopeptide cleavage by thrombin occurred within the first minutes, as is evident from the slight shift of the Aα and Bβ chains towards smaller molecular mass bands. The formation of γ-dimers already occurred in the first minutes, whereas higher molecular mass ligated chains formed more slowly. We quantified the relative amounts of the bands by using densitometry, which showed that the amount of γ-dimers increased rapidly in the first few minutes, and approached a plateau at ~ 5 min (Fig. 1B). In contrast, cross-linking of α-chains occurred only after 10 min, after which the amount of monomeric α-chains gradually decreased over the course of 4 h (Fig. 1C). We also monitored clot polymerization

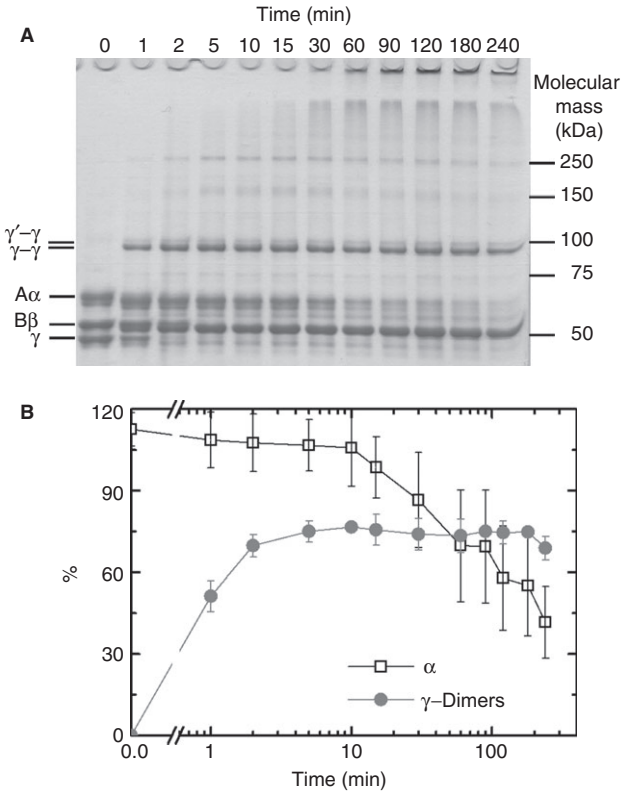

Fig. 1. Kinetics of formation of plasma-derived fibrin clots (2 mg mL^{-1} fibrin). (A) Reducing SDS-PAGE gel of plasma fibrin clot, where the reaction was terminated at the indicated time points. The bands corresponding to the α-chains, β-chains and γ-chains, as well as to the γ-dimers are indicated. Two populations of γ-dimers, corresponding to the γ–γ homodimers and γ′–γ heterodimers, were observed, as expected from the molecular heterogeneity of plasma fibrinogen. (B) Densitometry analysis was also performed to quantify the relative amounts of the non-cross-linked α-chains (open squares) and γ-dimers (filled circles). The percentages are normalized against the band density of β-chains in each lane. Error bars are standard deviations from multiple samples (n = 3).

mechanically by using rheology and visually by using turbidity. Interestingly, both G' and the turbidity showed rapid increases in the first 10 min of polymerization, followed by slow increases that did not fully cease after 4 h (Fig. 2A–B). Our observations are consistent with a recent study that also showed a slow increase in turbidity in the presence, but not in the absence, of FXIII [21]. We hypothesize that the continuous formation of higher-order-α-chain oligomers may underlie the slow increase in clot stiffness by playing a role in the lateral coupling of protofibrils within each fiber.

To test this hypothesis, we performed turbidimetric analysis during clot polymerization to probe the kinetics of protofibril lateral aggregation. As shown in Fig. 2D, the diameter of the fibrin fibers initially increased rapidly, reaching 203 ± 4 nm (n = 5) after 45 min, reflecting the lateral aggregation of protofibrils to form thick fibers. Strikingly, however, this phase was followed by a slow

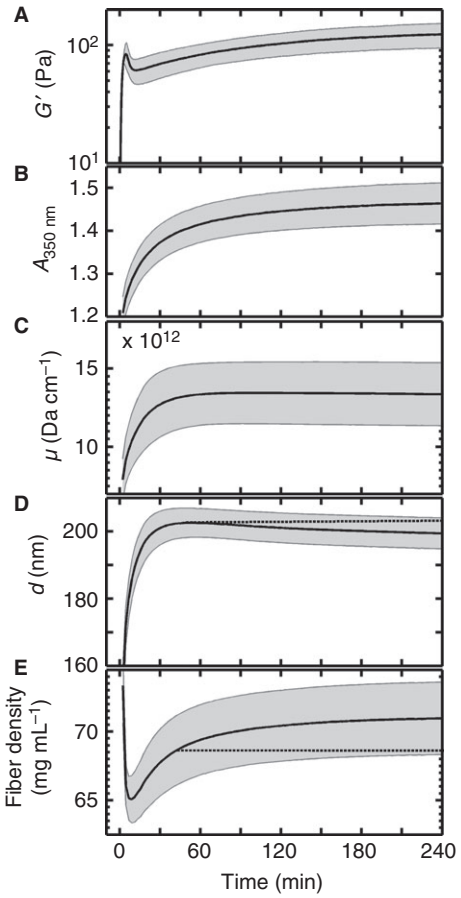

Fig. 2. Polymerization time course of plasma fibrin clots. The mechanical and structural properties of 2 mg mL^{-1} fibrin clots were monitored as a function of time after thrombin addition. Black lines denote the mean, and the shaded regions show the standard deviation. (A) The linear elastic modulus, G', was measured on fibrin clots polymerized *in situ* in the rheometer (n = 7). (B) The optical absorbance of self-assembling fibrin clots at 350 nm (n = 5). Turbidimetric analysis (see Materials and methods) was carried out to quantify the structure of fibrin fibers. (C–E) The mass/length ratio, μ (C), the average diameter, d (D), and the specific density (E) of the fibers are plotted as a function of time after the initiation of clotting (n = 5). The dotted lines in (D) and (E) are horizontal lines as guides for the eye.

but continuous decrease in the diameter. A decrease in fiber diameter has been qualitatively reported (based on confocal images), and speculated to arise from the fusion of multiple fibers [22]. Physically, fiber fusion would entail an increase in the mass/length ratio of the fiber. In contrast, we observed that the mass/length ratio was constant while the fiber diameter decreased (Fig. 2C). By combining the measured mass/length ratio and diameter, we can compute the specific density of the fibers, which represents how tightly the constituent protofibrils are packed together. The specific density of the fibers initially decreased in the first 20 min, owing to the continual addition of loosely coupled protofibrils onto existing fibers, but subsequently increased progressively (Fig. 2E). The slow decrease in fiber diameter that was accompanied by a corresponding slow increase in fiber density coincided with the progressive oligomerization of the α-chains. Our data therefore suggest that this oligomerization compacts the fibrin fibers. Furthermore, oligomerization coincided with the progressive stiffening of clots, suggesting that fibrin fiber compaction is responsible for this stiffening.

Inhibition of FXIII-induced cross-linking abrogates fiber compaction

To directly test the hypothesis that FXIII activity causes compaction of fibrin fibers, we added varying amounts of a specific inhibitor of FXIII activity, D004, to the self-assembling plasma-derived fibrin networks, which contain FXIII. SDS-PAGE analysis confirmed that increasing amounts of D004 resulted in decreasing amounts of covalent bonds (Fig. 3A). Addition of as little as 0.1 μM D004 abrogated the formation of high-molecular-mass α-chain oligomers, whereas at 200 μM D004, almost all α-chains and γ-chains remained non-cross-linked after 4 h of polymerization. To further study the clot structure and mechanical properties, we selected three D004 concentrations that represent qualitatively different regimes of cross-linking: 1 μM, where the high-molecular-mass oligomers (> 100 kDa) are much less abundant (< 10%) than in fully cross-linked clots; 10 μM, where the majority (> 75%) of cross-linking is γ-dimerization; and 200 μM, where almost all (> 95%) cross-linking is inhibited. Turbidimetry showed that FXIII inhibition did not affect the number of protofibrils per fiber, but increased the fiber diameter by ~ 20%, independently of D004 concentration (Fig. 3B). This suggests that the inhibition of the formation of high-molecular-mass chain oligomers abrogates fiber compaction, consistent with our hypothesis. Indeed, when we performed time-resolved turbidimetry on clots in the presence of 200 μM D004, we no longer observed a decrease in fiber diameter over time, and the specific density of the fibers quickly reached a plateau value (Fig. 3C). The final density of the fibers was 52 ± 2 mg mL^{-1}, which was significantly lower than the density (71 ± 3 mg mL^{-1}) found in the absence of D004 (P < 0.01).

To test whether FXIII inhibition also abrogates slow stiffening of the clots, we monitored the clot polymerization process by using rheology. As shown in Fig. 4A, G′ again increased rapidly in the first 10 min, but there was no longer a slow increase. Regardless of D004 concentration, the slow stiffening was absent. The final gel stiffness monotonically decreased with increasing D004 concentration (Fig. 4B). Changes in the macroscopic rheology could, in principle, result from changes at the fiber level and/or in the network architecture. To distinguish between these possibilities, we performed confocal fluorescence imaging of the clots under hydrated conditions (Fig. 6). Quantitative analysis of the confocal images indicated an average pore size of 1.6 ± 0.3 μm for cross-

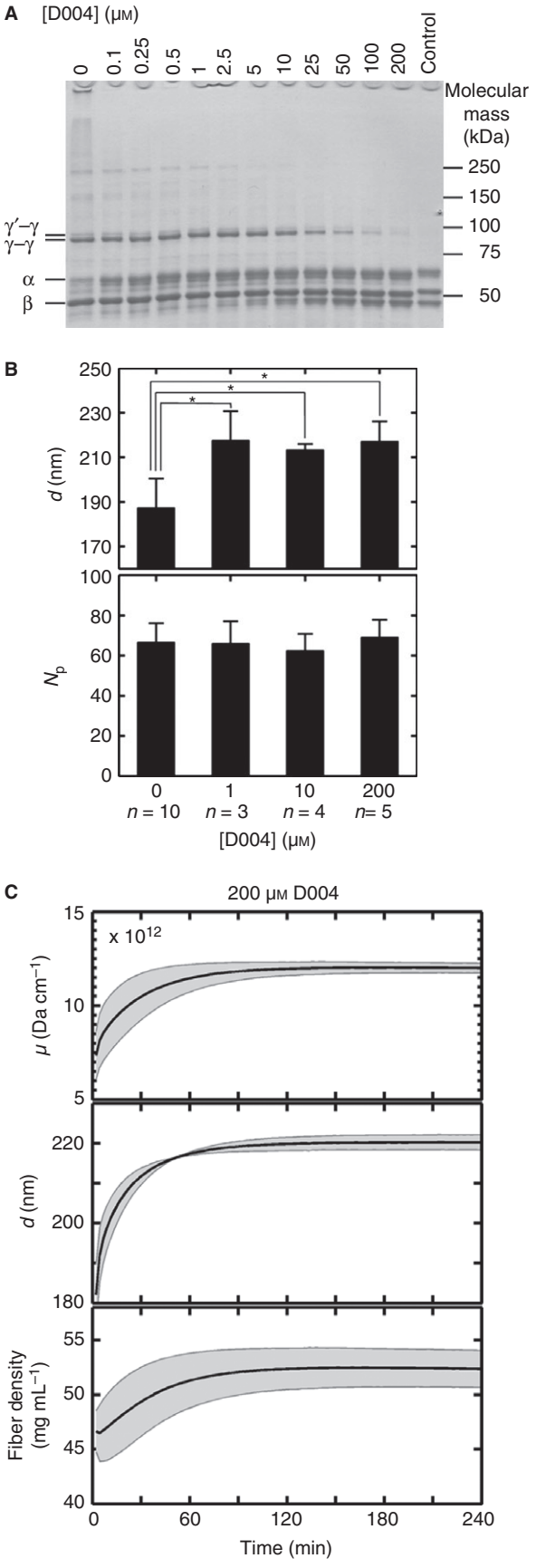

Fig. 3. Factor XIII inhibition abrogates fibrin fiber compaction. (A) Reducing SDS-PAGE gel of fibrin clots with increasing amounts of D004, an FXIII inhibitor. The extent of cross-linking gradually decreases with increasing concentration of D004, and at 200 μM cross-linking is completely inhibited (with 2 mg mL^{-1} fibrinogen; 4 h of incubation). As a control, the rightmost lane shows the bands corresponding to unclotted fibrinogen. (B) The average fiber diameter, d, is significantly affected ($^*P < 0.01$) by the presence of D004, but the number of protofibrils per fiber, N_p, is not. (C) Turbidimetry analysis revealed that the fiber mass/length ratio, μ, diameter, and specific density quickly approach constant values when fibrin cross-linking is inhibited with 200 μM D004, indicating the abrogation of slow fiber compaction. All samples contained 1% v/v dimethylsulfoxide. Data are mean ± standard deviation ($n \geq 3$).

linked plasma clots, which was not significantly affected by the addition of D004 (Fig. S3; $P > 0.4$). This is in agreement with previous quantifications of confocal reflectance [4] and scanning electron microscopy (SEM) [7] images, although a recent study reported a slight increase in the number density of fibers when FXIII was present, corresponding to an estimated decrease in pore size by 0.02 μm [13]. Taken together, these results support our hypothesis that FXIII-induced chain oligomerization compacts the fibers, and that this compaction stiffens the fibrin clot by stiffening the fibers.

Addition of FXIII to recombinant fibrin also leads to fiber compaction

Purified fibrinogen derived from plasma always contains heterogeneous molecular variants, because of genetic variations (splice variants and genetic polymorphisms), post-translational modifications (glycosylation, phosphorylation, and sulfation), proteolysis-induced variations, and copurified plasma proteins such as FXIII [23]. These factors probably play a role in fibrin clotting, and could potentially influence our observation of fiber compaction. To rule out any other factors present in the plasma-derived fibrinogen that may, for example, interact with D004 and affect the results, we also performed experiments with rFib610. The kinetics of fibrinopeptide release and clotting of rFib610 are comparable to those of plasma fibrinogen [24].

SDS-PAGE analysis showed no cross-linked chains without the addition of exogenous FXIII, confirming the absence of FXIII in rFIb610 (Fig. 5A). Addition of increasing amounts of FXIII increased the degree of cross-linking in the rFib610 clot (Fig. 5A). The formation of γ-dimers was first visible on the gel at an FXIII concentration of 0.05 μg mL^{-1}, and was complete (within 4 h of incubation) at 1 μg mL^{-1}. Higher molecular mass complexes formed when the FXIII concentration was further raised, until the extent of cross-linking became comparable to that in fully cross-linked plasma fibrin with the addition of 20 μg mL^{-1} FXIII. The stiffness of the clot

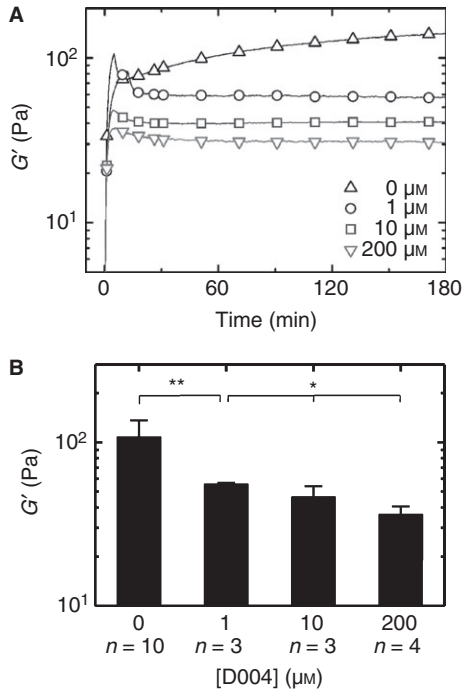

Fig. 4. The effect of factor XIII on clot mechanical properties. (A) The elastic modulus (G') of 2 mg mL^{-1} fibrin clots in the first 3 h of polymerization in the presence of 0, 1, 10 and 200 μM D004, showing that inhibition of FXIII-mediated cross-linking abolishes the slow increase in G' after the first ~ 30 min. (B) The clot stiffness decreases with increasing D004 concentration (**$P < 0.015$; *$P < 0.1$).

increased monotonically with increasing FXIII concentration (Fig. 5B). At 20 μg mL^{-1} FXIII, the stiffness was four-fold higher than in the absence of FXIII and comparable to that of plasma fibrin. The evolution of G' as a function of time during polymerization showed a similar trend as for plasma fibrin: the slow increase in G' was observed when FXIII was present, but not when FXIII was absent (Figs 5C and S4). Characterization of the fibers with time-resolved turbidimetry also showed similar trends as for plasma fibrin: fiber compaction occurred with FXIII but not in the absence of FXIII (Fig. 5D). The final fiber specific density was ~ 35% higher in the presence of FXIII than in its absence. Confocal microscopy revealed no significant difference in the network structure of rFib610 clots with and without FXIII (Fig. 6). These findings are all consistent with our earlier conclusions in the case of plasma fibrin clots, strongly suggesting that FXIII-mediated formation of covalent bonds causes fiber compaction and stiffens networks by stiffening the constituent fibers.

Clot behavior at large stresses

The next question we asked was whether fiber compaction and stiffening also affect clot behavior at large deformations. This is especially important to consider, as fibrin clots are continually subjected to high dynamic shear stresses because of blood flow [25] and static stress because of platelet contraction [26]. It has been known for decades that blood clots and purified fibrin networks become stiffer as they are increasingly stretched – a phenomenon called strain (or stress) stiffening – thereby maintaining their mechanical integrity against premature rupture [27,28].

The measured differential stiffness, K', for plasma clots (with and without D004) and for recombinant clots (with and without FXIII) are plotted as a function of increasing applied prestress in Fig. 7. Consistent with prior reports, K' increased with the applied stress above a certain critical stress. At the same fibrin concentration, cross-linked clots showed a larger K' in the linear region (i.e. up to a critical stress of ~ 5 Pa) than non-cross-linked clots, for both plasma-derived and recombinant fibrins. This clearly indicates the vital role of FXIII in governing the mechanics of fibrin clots. However, in the non-linear regime at stresses beyond the critical stress, the stress responses of the four clots were almost indistinguishable. These results suggest that, once the clot is sufficiently stressed, the internal molecular packing of the individual fibrin fibers no longer plays an important role in the network behavior.

Discussion

In this study, we have presented evidence that FXIII-mediated cross-linking plays a role in clot maturation by compacting fibrin fibers. This fiber compaction results in stiffer clots, although the network structure is not significantly affected. The compaction occurs through the formation of cross-links between the protofibrils within each fiber, and is suppressed when FXIII activity is inhibited. Furthermore, the slow increase in the clot stiffness, which we have shown to be the mechanical signature of fiber compaction, is only observed in the presence of active FXIII. This fiber compaction process may explain the recent observation that clots form thinner fibers in the presence of FXIII [13]. On the basis of these results, we propose a working model whereby the maturation of fibrin fibers in cross-linked clots involves quick end-to-end cross-linking of the γ-chains and slow α-chain oligomerization that accompanies lateral aggregation of protofibrils (Fig. 8). The exact molecular identity and spatial arrangement of the high molecular mass oligomers remain to be established. FXIII-aided formation of γ-chain trimers and tetramers [29], α-chain multimers up to 770 kDa [30] and α–γ hybrid polymers [18,31] has been reported, although the time scale on which these processes occur and the effects on fiber morphology are unclear. It is plausible, nevertheless, that the initial stages in the lateral protofibril aggregation bring together protofibrils with sparse linkages, creating a loosely packed and floppy fiber, and, as higher-molecular-mass chain oligomers continue to progressively form, the fibers become more densely packed, compact, and rigid.

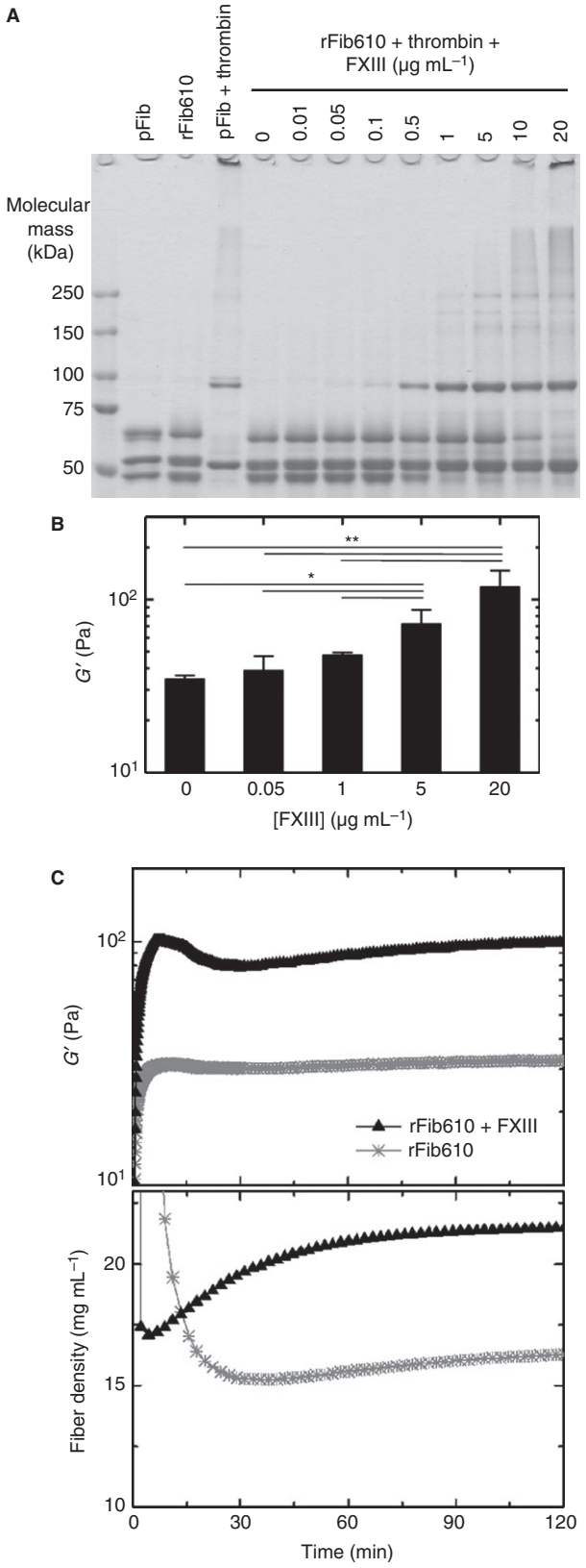

Fig. 5. Factor XIII affects the structure and mechanical properties of recombinant (recombinant fibrinogen [rFib610]) fibrin clots. (A) Reducing SDS-PAGE gel of rFib610 and fibrin with different amounts of FXIII, with plasma fibrinogen (pFib) as comparison. Complete ligation is observed with the addition of 20 μg mL^{-1} FXIII (at 2 mg mL^{-1} fibrinogen; 4 h of incubation), as shown by the disappearance of the bands representing the α-chain and γ-chain monomer species, and the similar degree of cross-linking as in the plasma-derived fibrin clot. (B) The stiffness of the clots, as measured by the elastic modulus, G', after 4 h of polymerization, increases with FXIII concentration (**$P < 0.05$; *$P < 0.1$). (C) The evolution of G' after the initiation of polymerization of rFib610 clots without and with 20 μg mL^{-1} FXIII. There is a slow increase in G' in the presence, but not in the absence, of FXIII. (D) The evolution of the specific density of the fibers in the first 2 h of polymerization.

FXIII-mediated fiber compaction has several testable and clinically relevant consequences. First, the bending stiffness of individual fibrin fibers should gradually increase as the fibers mature. Fibrin fibers are essentially bundles of semiflexible protofibrils. Models of semiflexible polymer bundles predict that the bending stiffness of a bundle should increase proportionally with the number of constituent polymers, N_p, when the polymers are loosely coupled, and with N_p^2 in the case of tight coupling [32]. The chain oligomerization and fiber compaction resulting from FXIII-mediated cross-linking reported here imply that the protofibril coupling becomes tighter as the fibers mature. Indeed, we found that inhibition of FXIII-mediated cross-linking resulted in more loosely coupled protofibrils from a theoretical analysis of clot stiffness in terms of a semiflexible bundle model [33] (Fig. S5). A recent SEM study of mature fibrin networks also showed that the fibers appear straighter when FXIII is present [21], further supporting the idea that fiber compaction results in stiffer individual fibers. It is conceivable that fiber tightening plays an important role during thrombus formation and development, because, as the thrombus grows in size, the fibrin fibers are subjected to increasing shear forces. The compaction and stiffening of the fibers can thus help in resisting excessive deformation and damage.

Whereas FXIII has a pronounced effect on the low-strain modulus of fibrin clots, the high-strain modulus is independent of cross-linking. This finding suggests that different deformation mechanisms are at work at different levels of stress. At small stresses, the clot response is governed by the thermal bending fluctuations of the fibers [14], which are, in turn, dependent on how tightly the constituent protofibrils are coupled together. However, once the clot is sufficiently stressed, the modulus is governed by the stretch modulus of the fibers. If all protofibrils are simply stretched in parallel, the stretch modulus is independent of the degree of coupling. Moreover, there is evidence that fibers expel water and collapse at large strain [34]. At this point, the network response is expected to be governed by the intrinsic mechanics of single protofibrils, so that lateral coupling no longer plays an important role (Fig. 8). As a simple test for this model, we performed prestress measurements on plasma-derived fibrin clots at different time points (i.e. 10 min,

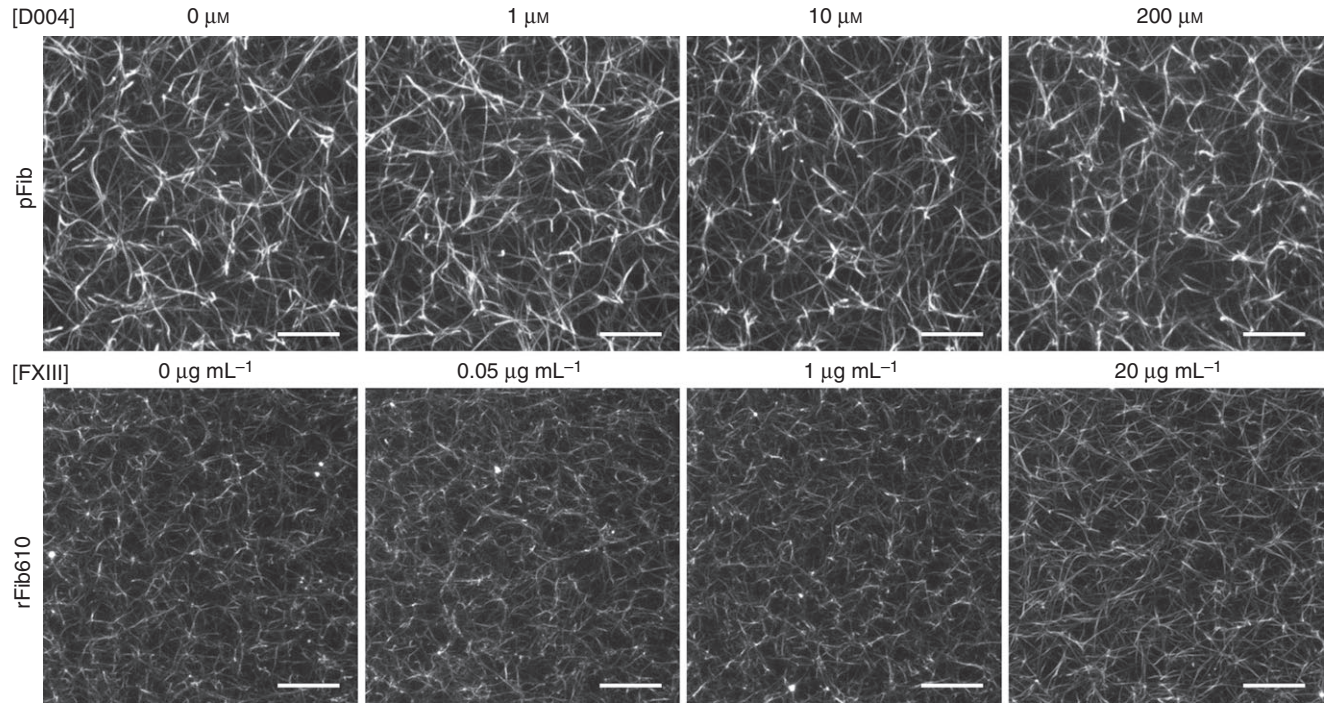

Fig. 6. Confocal fluorescence images of plasma-derived (plasma fibrinogen [pFib]; upper panel) and recombinant (recombinant fibrinogen [rFib610]; lower panel) fibrin clots, polymerized with different amounts of the FXIII inhibitor D004 for the former and of exogenous FXIII for the latter. Images are z-projections of 129 frames over a 25.6-μm-thick section of the network. Scale bars: 10 μm.

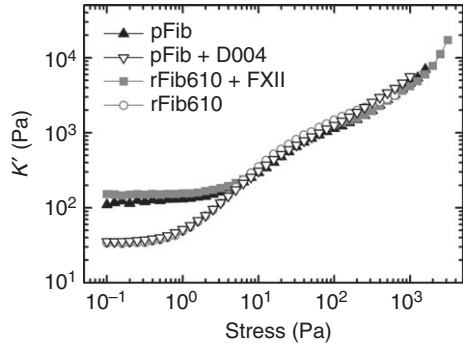

Fig. 7. The non-linear elastic response of ligated and unligated fibrin clots. The differential elastic modulus (K') is plotted as a function of applied shear stress for a 2 mg mL^{-1} plasma fibrin clot (plasma fibrinogen [pFib]) in the absence and presence of 200 μM D004, and for a 2 mg mL^{-1} recombinant fibrin clot (recombinant fibrinogen [rFib610]) in the absence and presence of 20 μg mL^{-1} FXIII.

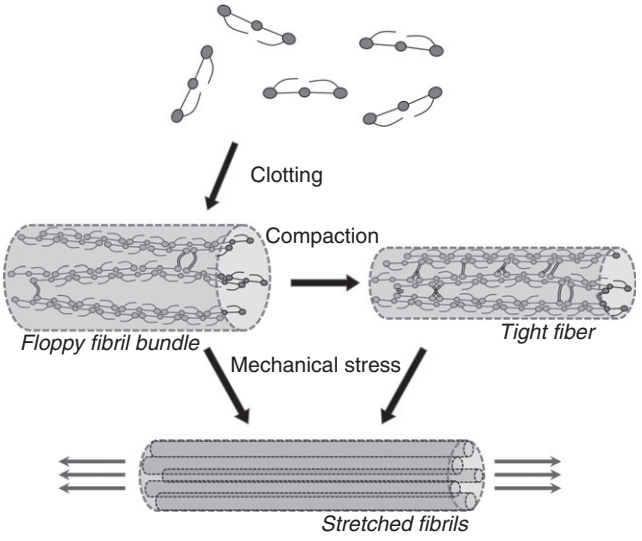

Fig. 8. Structural model of the coupling between protofibrils within fibrin fibers. Clotting starts with the assembly of protofibrils that aggregate laterally to form sparsely cross-linked, floppy fibers within the fibrin network. As FXIII-mediated cross-linking between the α-chains and γ-chains (depicted by double lines) becomes more extensive and complex, the fibers mature as tightly coupled fibril bundles with a smaller diameter and higher protein density, and therefore smaller intrafibrillar pores. Under large stresses, however, the clot mechanical properties are governed by the intrinsic properties of the individual fibrils.

1 h, and 4 h) after the initiation of polymerization. In this case, we expect the clot stiffness to be still evolving with time at small stresses, but not to be affected at large stresses. Indeed, we found that the small-stress modulus gradually increased with time, but the stiffness curves completely overlapped each other at large stresses (Fig. S6).

Our study reveals an important aspect of fibrin clots that has previously received little attention, namely the intrafibrillar structure. Although cross-linking by FXIII does not significantly affect the structure at the network level, it considerably alters the structure within the fibers through chain oligomerization and fiber compaction. The tightness of coupling between protofibrils making up the fiber bundle determines the size of pores in the fibers,

which can affect the rates of molecular diffusion through the fibers. This can in turn affect fibrinolysis. For example, lysis agents such as plasmin are believed to freely diffuse through pores within the fiber [35]. Consequently, tightening of the intrafibrillar pores because of both cross-link maturation and stress-induced fiber compaction can restrict diffusion of these molecules, impede access to the degradation sites in the coiled-coil region between the D-domains and E-domains, and slow down lysis. Indeed, the presence of FXIII has been recently shown to slow fibrinolysis even in the absence of bound α_2-antiplasmin [13,21]. Furthermore, clot age [36], increased complexity of α-chain cross-linking [37] and mechanical stress/strain [38,39] have all been shown to endow fibrin with increased resistance to lysis. Additionally, FXIII-induced fiber compaction may also hide or expose binding sites for growth factors and clot components that are responsible for cell attachment [40], thus potentially making this process important in wound healing and hemostatic progression.

Addendum

N. A. Kurniawan designed and performed the experiments, analyzed data, and wrote the manuscript. J. Grimbergen and J. Koopman assisted in study design, contributed materials and reagents, and reviewed the manuscript. G. H. Koenderink supervised the work, assisted in study design, analyzed data, and wrote the manuscript.

Acknowledgements

The authors thank I. Piechocka, J. Weisel, F. Caton, B. Polack, B. Vos and K. Jansen for useful discussions. This work is part of the Industrial Partnership Programme (IPP) of the Stichting voor Fundamenteel Onderzoek der Materie (FOM), which is financially supported by the Nederlandse Organisatie voor Wetenschappelijk Onderzoek (NWO), and was further supported by a Marie Curie IIF fellowship awarded to N. A. Kurniawan.

Disclosure of Conflict of Interests

J. Grimbergen and J. Koopman are current employees of ProFibrix, part of The Medicines Company. N. A. Kurniawan and G. H. Koenderink state that they have no conflict of interest.

Supporting Information

Additional Supporting Information may be found in the online version of this article:

Fig. S1. Turbidimetry measurements of non-cross-linked 2 mg mL^{-1} rFib610 networks containing either FXIII inhibitor (200 μM D004; blue solid line) or vehicle (1% v/v DMSO; red dashed line).

Fig. S2. Turbidimetry analysis. (A) Typical raw turbidity (τ), plotted as a function of wavelength (λ) and time for a 2 mg mL^{-1} plasma-derived fibrin sample.

Fig. S3. Quantitative analysis of network pore size from confocal images.

Fig. S4. The effect of factor XIII on the polymerization of fibrin clots.

Fig. S5. Tightness of coupling between protofibrils within fibrin fibers.

Fig. S6. Non-linear rheology of 2 mg mL^{-1} plasma-derived fibrin clot as a function of clot age.

References

1 Weisel JW, Litvinov RI. Mechanisms of fibrin polymerization and clinical implications. *Blood* 2013; **121**: 1712–19.
2 Ariëns RAS, Lai TS, Weisel JW, Greenberg CS, Grant PJ. Role of factor XIII in fibrin clot formation and effects of genetic polymorphisms. *Blood* 2002; **100**: 743–54.
3 Shen L, Lorand L. Contribution of fibrin stabilization to clot strength. Supplementation of factor XIII-deficient plasma with the purified zymogen. *J Clin Invest* 1983; **71**: 1336–41.
4 Collet J-P, Shuman H, Ledger RE, Lee S, Weisel JW. The elasticity of an individual fibrin fiber in a clot. *Proc Natl Acad Sci USA* 2005; **102**: 9133–7.
5 Karimi M, Bereczky Z, Cohan N, Muszbek L. Factor XIII deficiency. *Semin Thromb Hemost* 2009; **35**: 426–38.
6 Weisel JW. The mechanical properties of fibrin for basic scientists and clinicians. *Biophys Chem* 2004; **112**: 267–76.
7 Ryan EA, Mockros LF, Weisel JW, Lorand L. Structural origins of fibrin clot rheology. *Biophys J* 1999; **77**: 2813–26.
8 Liu W, Carlisle CR, Sparks EA, Guthold M. The mechanical properties of single fibrin fibers. *J Thromb Haemost* 2010; **8**: 1030–6.
9 Helms CC, Ariens RA, de Uitte Willige S, Standeven KF, Guthold M. a–a Cross-links increase fibrin fiber elasticity and stiffness. *Biophys J* 2012; **102**: 168–75.
10 Yeromonahos C, Polack B, Caton F. Nanostructure of the fibrin clot. *Biophys J* 2010; **99**: 2018–27.
11 Radulovic V, Baghaei F, Blixter IF, Samuelsson S, Jeppsson A. Comparable effect of recombinant and plasma-derived human fibrinogen concentrate on ex vivo clot formation after cardiac surgery. *J Thromb Haemost* 2012; **10**: 1696–8.
12 Freund KF, Doshi KP, Gaul SL, Claremon DA, Remy DC, Baldwin JJ, Pitzenberger SM, Stern AM. Transglutaminase inhibition by 2-[(2-oxopropyl)thio]imidazolium derivatives: mechanism of factor XIIIa inactivation. *Biochemistry* 1994; **33**: 10109–19.
13 Hethershaw EL, Cilia La Corte AL, Duval C, Ali M, Grant PJ, Ariëns RA, Philippou H. The effect of blood coagulation factor XIII on fibrin clot structure and fibrinolysis. *J Thromb Haemost* 2014; **12**: 197–205.
14 Piechocka IK, Bacabac RG, Potters M, MacKintosh FC, Koenderink GH. Structural hierarchy governs fibrin gel mechanics. *Biophys J* 2010; **98**: 2281–9.
15 Carr ME Jr, Shen LL, Hermans J. Mass–length ratio of fibrin fibers from gel permeation and light scattering. *Biopolymers* 1977; **16**: 1–15.
16 De Spirito M, Arcovito G, Papi M, Rocco M, Ferri F. Small- and wide-angle elastic light scattering study of fibrin structure. *J Appl Crystallogr* 2003; **36**: 636–41.
17 Carr ME Jr, Hermans J. Size and density of fibrin fibers from turbidity. *Macromolecules* 1978; **11**: 46–50.

18 Ryan EA, Mockros LF, Stern AM, Lorand L. Influence of a natural and a synthetic inhibitor of factor XIIIa on fibrin clot rheology. *Biophys J* 1999; **77**: 2827–36.
19 Mosesson MW. Short by one mechanism: a rebuttal. *J Thromb Haemost* 2010; **8**: 2089–90.
20 Guthold M, Carlisle C. Single fibrin fiber experiments suggest longitudinal rather than transverse cross-linking: reply to a rebuttal. *J Thromb Haemost* 2010; **8**: 2090–1.
21 Duval C, Allan P, Connell SD, Ridger VC, Philippou H, Ariëns RA. Roles of fibrin α- and γ-chain specific cross-linking by FXIIIa in fibrin structure and function. *Thromb Haemost* 2014; **111**: 842–50.
22 Collet J-P, Lesty C, Montalescot G, Weisel JW. Dynamic changes of fibrin architecture during fibrin formation and intrinsic fibrinolysis of fibrin-rich clots. *J Biol Chem* 2003; **278**: 21331–5.
23 de Maat MP, Verschuur M. Fibrinogen heterogeneity: inherited and noninherited. *Curr Opin Hematol* 2005; **12**: 377–83.
24 Raynal B, Cardinali B, Grimbergen J, Profumo A, Lord ST, England P, Rocco M. Hydrodynamic characterization of recombinant human fibrinogen species. *Thromb Res* 2013; **132**: e48–53.
25 Campbell RA, Aleman M, Gray LD, Falvo MR, Wolberg AS. Flow profoundly influences fibrin network structure: implications for fibrin formation and clot stability in haemostasis. *Thromb Haemost* 2010; **104**: 1281–4.
26 Lam WA, Chaudhuri O, Crow A, Webster KD, Li TD, Kita A, Huang J, Fletcher DA. Mechanics and contraction dynamics of single platelets and implications for clot stiffening. *Nat Mater* 2011; **10**: 61–6.
27 Janmey PA, Winer JP, Weisel JW. Fibrin gels and their clinical and bioengineering applications. *J R Soc Interface* 2009; **6**: 1–10.
28 Storm C, Pastore JJ, MacKintosh FC, Lubensky TC, Janmey PA. Nonlinear elasticity in biological gels. *Nature* 2005; **435**: 191–4.
29 Mosesson MW, Siebenlist KR, Amrani DL, DiOrio JP. Identification of covalently linked trimeric and tetrameric D domains in crosslinked fibrin. *Proc Natl Acad Sci USA* 1989; **86**: 1113–17.
30 Francis CW, Marder VJ. Rapid formation of large molecular weight α-polymers in cross-linked fibrin induced by high factor XIII concentrations. Role of platelet factor XIII. *J Clin Invest* 1987; **80**: 1459–65.
31 Shainoff JR, Urbanic DA, DiBello PM. Immunoelectrophoretic characterizations of the cross-linking of fibrinogen and fibrin by factor XIIIa and tissue transglutaminase. Identification of a rapid mode of hybrid α-/γ-chain cross-linking that is promoted by the γ-chain cross-linking. *J Biol Chem* 1991; **266**: 6429–37.
32 Claessens MMAE, Bathe M, Frey E, Bausch AR. Actin-binding proteins sensitively mediate F-actin bundle stiffness. *Nat Mater* 2006; **5**: 748–53.
33 Piechocka IK, Jansen KA, Broedersz CP, MacKintosh FC, Koenderink GH. Semiflexible bundle model explains the elasticity of fibrin networks. *arXiv* 2012. 1206.3894v1.
34 Brown AEX, Litvinov RI, Discher DE, Purohit PK, Weisel JW. Multiscale mechanics of fibrin polymer: gel stretching with protein unfolding and loss of water. *Science* 2009; **325**: 741–4.
35 Weisel JW, Litvinov RI. The biochemical and physical process of fibrinolysis and effects of clot structure and stability on the lysis rate. *Cardiovasc Hematol Agents Med Chem* 2008; **6**: 161–80.
36 Weisel JW. Stressed fibrin lysis. *J Thromb Haemost* 2011; **9**: 977–8.
37 Gaffney PJ, Whitaker AN. Fibrin crosslinks and lysis rates. *Thromb Res* 1979; **14**: 85–94.
38 Varjú I, Sótonyi P, Machovich R, Szabó L, Tenekedjiev K, Silva MMCG, Longstaff C, Kolev K. Hindered dissolution of fibrin formed under mechanical stress. *J Thromb Haemost* 2011; **9**: 979–86.
39 Adhikari AS, Mekhdjian AH, Dunn AR. Strain tunes proteolytic degradation and diffusive transport in fibrin networks. *Biomacromolecules* 2012; **13**: 499–506.
40 Grinnell F, Feld M, Minter D. Fibroblast adhesion to fibrinogen and fibrin substrata: requirement for cold-insoluble globulin (plasma fibronectin). *Cell* 1980; **19**: 517–25.